Ultrasound assisted modification of graphite felt with electroless silver – Part 1: composition, morphology, structure and electrical conductivity

Brigita Macijauskienė*,

Egidijus Griškonis

*Department of Physical
and Inorganic Chemistry,
Kaunas University of Technology,
Radvilėnų Rd. 19,
LT-50254 Kaunas, Lithuania*

The influence of ultrasound action on the modification of graphite felt with the electroless Ag was investigated. It has been gravimetrically estimated that mass fraction (wt.%) of Ag loaded on the surface of graphite felt filaments depends on the ultrasonic impact. The mass fraction of electroless-deposited Ag on the graphite felt filaments in the presence of ultrasound action is 1.6 times higher than the one of graphite felt modified without ultrasound action. The morphology, composition and structure of the internal and external filaments of graphite felt samples modified in the absence and presence of ultrasound action were determined by scanning electron microscopy (SEM), energy dispersive X-ray spectroscopy (EDX) and X-ray diffraction (XRD), respectively. It was found that a more uniform distribution of Ag particles in the whole volume of the graphite felt sample took place when ultrasonication of electroless Ag deposition solution was used. The nanaocrystaline Ag with an average crystallite size of 14 nm was deposited on the surface of graphite felt filaments in the absence of ultrasound action. Meanwhile, the crystallite size of electroless Ag slightly decreased to approximately 11 nm when ultrasonication was used during the deposition process. Uniform deposition of Ag particles of nanometric dimensions in the graphite felt matrix increased the electrical conductivity up to 10.7 S cm^{-1}, and this value is about 1.6 times higher in comparison with conductivity of a bare graphite felt.

Key words: graphite felt, modification, electroless Ag, ultrasonication, conductivity

INTRODUCTION

Porous electrodes have found a great deal of applications in the field of electrochemistry, ranging from fuel cells [1] to electrochemical synthesis of organic compounds [2]. In the light of constantly increasing demands for material properties and applications of porous electrodes, novel and highly promising materials such as graphite felt (GF) are introduced. GF is obtained by thermally treating polyacrylonitrile (PAN) felt in an inert gas atmosphere. During carbonization and graphitization processes at high temperature PAN macromolecules convert into a graphite structure possessing a carbon atom skeleton – GF [3]. The material has high surface area, thermal and chemical resistance, is particularly light (density is about 0.1 g · cm^{-3}) [4] and most importantly – possesses a relatively high electrical conductivity, i. e. low resistivity. Electrical resistivity of GF varies in the range from 10^{-2} to 10^{-1} Ω · m [4–5]. These qualities are extremely useful for application of GF not only as a porous electrode in many electrochemical devices (fuel cells, flow batteries, electrochemical synthesis reactors, etc.) but also for retrieval of metals from spent fixing baths [6] and oxidation of harmful organic compounds in waste water [7].

However, unique properties of GF enable it to serve as a substrate for modification in order to obtain different electrode compositions. Modification of GF through the use of various metals greatly improves application prospects for GF electrodes. For example, GF electrodes modified with iron group metals (Ni, Co) exhibit electro-catalytic properties when performing reverse electrochemical oxidation-reduction processes of sulfide and poly-sulfide anions, in sodium poly-sulfide / bromine redox flow batteries [8]. Furthermore, GF modified with Ni, Co and Ni-Co alloy provides a cheaper alternative for reducing overall potential and increasing catalytic activity in the hydrogen evolution reaction [9]. The modification of GF with some noble metals or their alloys, especially in the nanometric scale, could lead to use of such compositions as flow-through electrodes in fuel cells [10–12] in all-vanadium flow batteries [13–15], for catalytic synthesis of some

---

* Corresponding author. E-mail: brigita.macijauskiene@ktu.edu

compounds [2, 16] and as electrochemical sensors of the target substances [17].

Meanwhile, Ag, as an electrode, exhibits electro-catalytic properties through dehalogenation of several classes of halides [18]. However, research has suggested that there is high potential in micro- and nanostructured Ag to exhibit similar or even higher electro-catalytic activity than their polycrystalline bulk counterparts in some oxidation-reduction reactions [19]. Catalytic and autocatalytic reduction of hydrogen peroxide on flat and nano-porous Ag electrodes was comprehensively investigated in both acidic [20] and alkaline solutions [21]. Synthesis of a carbon supported Ag electro-catalyst is widely investigated due to possible application as a cathode material in alkaline polymer electrolyte membrane fuel cells [22, 23]. In addition, newly emerging research has shown that nano-porous Ag has great potential for selectively converting CO_2 into CO, which is a useful concept to aiding the environmental cause [24].

As far as ultrasound usage in chemistry is concerned, two research areas are most highlighted – sonochemistry and sonoelectrochemistry. The main phenomenon in both areas is acoustic cavitation, which results in the initiation or enhancement of the chemical activity of reacting species and mass transport in the liquid phase or in the interface of liquid–solid phases, e. g. at the surface of electrode [25]. Therefore, chemical and electrochemical synthesis of different materials could be significantly accelerated by ultrasound assistance or it could result in new reaction mechanisms [26]. In the recent years, there has been a considerable interest in the production of various nanomaterials through the use of sonochemistry and sonoelectrochemistry techniques [26–28]. Ultrasound assisted modification of some non-conducting polymeric materials with electroless-deposited Ag nanoparticles has been reported as well [29].

The aim of this study was to investigate the influence of ultrasonic irradiation on electroless-deposited Ag distribution in external and internal parts of graphite felt samples through investigation of changes in the structure, morphology, composition, and electrical conductivity of this microfiber material. In comparison, the above-mentioned characteristics were also determined for bare graphite felt and for graphite felt samples modified with electroless-deposited Ag in the absence of ultrasonic irradiation.

EXPERIMENTAL

The graphitized polyacrylonitrile fiber felt, simply named as graphite felt (GF), purchased from Wale Apparatus (USA) was used in this work. GF samples of 25 ± 0.5 mm length and 10 ± 0.5 mm width were cut out from a GF sheet of 4 ± 0.2 mm thickness. All chemicals of an analytically pure grade were purchased from Reakhim, Sigma-Aldrich and Lachema. Double-distilled water with the specific conductivity less than 0.5 µS cm^{-1} was used throughout the present study as a solvent. All experiments were carried out at room temperature (20 ± 1 °C). An ultrasonic bath VTUSC3 (Vellman)

with ultrasound frequency of 42 kHz was used to improve pre-treatment and modification processes.

The modification of GF samples with Ag was carried out by using the electroless deposition process [30], immediately after alkali-acid pre-treatment in 1 M NaOH and 1 M HCl solutions. Two separate aqueous solutions **A** and **B** were prepared for electroless Ag deposition. Solution **A** was a source of Ag$^+$ ions and contained 0.25 M AgNO$_3$, 0.5 M KOH and a proper quantity of concentrated ammonia solution for a complete dissolution of formed Ag$_2$O (pH > 13). Solution **B** contained 0.25 M *D*-glucose as the reducing agent. GF modified with Ag in the absence and presence of ultrasound action, hereinafter referred to as GF-Ag and GF-Ag-US, respectively. The sequence, conditions and durations of each pre-treatment and electroless Ag deposition procedure are described in detail, in the Results and Discussion.

The loading of electroless-deposited Ag on the surface of GF filaments is expressed by the mass fraction of Ag (w_{Ag}, wt.%) which was calculated after a gravimetrical analysis according to the following equation:

$$w_{Ag} = \frac{m - m_o}{m} \cdot 100\%,$$

where m_o and m are masses of the GF sample before and after alkali-acid pre-treatment and modification with electroless Ag, respectively. Mass determination was performed with a weighing accuracy of ±0.0001 g using an analytical balance ABJ 120-4M (Kern).

Investigations of the surface morphology, elemental composition and structure of filaments in the external and internal parts of GF-Ag and GF-Ag-US samples were performed after proper splitting of the samples. In order to avoid the influence of external filaments on the investigation of internal ones and vice versa, the external layers of GF-Ag and GF-Ag-US samples were separated from the internal layer using a scalpel trimming.

Surface morphology and composition of GF-Ag and GF-Ag-US filaments were investigated with a Qanta FEG 200 (FEI) high resolution scanning electron microscope (SEM) equipped with a Bruker XFlash® 4030 detector (Bruker AXS) for high resolution energy dispersive X-ray spectroscopy (EDX).

The structure of bare GF, GF-Ag and GF-Ag-US was investigated by means of X-ray diffraction (XRD). XRD measurements were performed with a Bruker D8 Advance (Bruker AXS) diffractometer in the 2θ range from 10° to 70° and with Ni-filtered CuK_a radiation (λ = 1.54056 10^{-10} m). The voltage and current of the X-ray tube was 40 kV and 40 mA, respectively. In accordance with the X-ray data of the diffraction patterns, in bare GF, GF-Ag and GF-Ag-US presented phases were identified using the software EVA (Bruker AXS) and PDF-2 database. The calculation of the crystallite size of electroless-deposited Ag was performed in the conventional way, according to the Scherrer formula [31], after the measurements of full widths at the half maxima (FWHM) of the characteristic peaks observed in the X-ray diffraction patterns by using the free access software XFIT.

The electrical conductivity of GF-Ag and GF-Ag-US, and for comparison of bare GF, was determined by measurement of the differential conductance dI/dE of rectangular samples with the above specified dimensions according to the methodology described in [32]. This was done by connecting to the ends of sample clips made from silvered copper foil and recording voltammetric characteristics of each sample. The current–voltage (I–E) curves were recorded by applying the cyclic voltammetry technique in the potential range from –1 V to +1 V at the sweep rate 100 mV s^{-1} using the above mentioned potentiostat-galvanostat. The calculation of the conductivity σ of GF and GF-Ag samples was performed according to the formula:

$$\sigma = \frac{L}{a \cdot b} \cdot \left(\frac{dI}{dE} \right),$$

where L is the distance between the two silvered copper foil clips; a, b are the width and the thickness of the samples, respectively; the differential conductance dI/dE corresponds to the slope of the recorded I–E curves which have a straight line form.

RESULTS AND DISCUSSION

GF pre-treatment and modification with Ag

Throughout the experiments it has been observed that GF is hydrophobic as it hardly got wet when it was exposed to the water based solutions. Literature data [8, 33] refers to the exposure of GF from 40 min to 1 h in the boiling aqueous NaOH solution in order to increase hydrophilicity of GF filaments. At the same time, the exposure of GF in hot or boiling oxidizing inorganic oxoacids (HNO$_3$ or H$_2$SO$_4$, as well as their mixture) greatly increases the concentration of C–O and C=O functional groups on the surface of GF filaments [34]. Therefore, in order to increase hydrophilicity of GF without increasing concentration of oxygen possessing functional groups on the surface of GF filaments, the following pre-treatment operations of the GF filaments surface, i. e. hydrophilization, were introduced before further modification with electroless Ag:

1) Wetting in 1 M NaOH solution while simultaneously exposing to ultrasound (up to 3 min) and further boiling in this solution for up to 1 h;
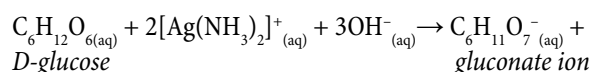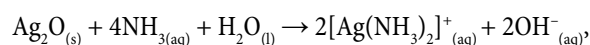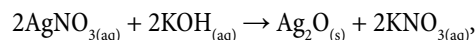
2) Rinsing with distilled water while simultaneously exposing to ultrasound (for at least 3 times, each rinsing taking up to 3 min, each time with a new portion of approximately 50 cm^3 of distilled water);

3) Boiling in 1 M HCl solution for up to 1 h;

4) Rinsing with distilled water while simultaneously exposing to ultrasound (until neutral reaction of rinsing water, each rinsing lasts up to 3 min, each time with a new portion of approximately 50 cm^3 of distilled water).

After the above-mentioned alkali-acid pre-treatment procedures, a hydrophilized GF sample was impregnated in 10 cm^3 of the solution **A** while simultaneously being exposed to ultrasonication for 6 min. Then, an equal volume of the so-

lution **B** was added to the solution **A** and electroless Ag deposition on the surface of GF filaments started to take place. It lasted for another 3, 6, 12 and 24 minutes under ultrasound action. The processes taking place in the solution **A** during its preparation and electroless Ag deposition process occurring after mixing of the solutions **A** and **B** could be described by the following reaction equations:

$$2AgNO_{3(aq)} + 2KOH_{(aq)} \rightarrow Ag_2O_{(s)} + 2KNO_{3(aq)},$$

$$Ag_2O_{(s)} + 4NH_{3(aq)} + H_2O_{(l)} \rightarrow 2[Ag(NH_3)_2]^{+}_{(aq)} + 2OH^{-}_{(aq)},$$

$$C_6H_{12}O_{6(aq)} + 2[Ag(NH_3)_2]^{+}_{(aq)} + 3OH^{-}_{(aq)} \rightarrow C_6H_{11}O_{7}^{-}{}_{(aq)} +$$
$$\text{\textit{D-glucose}} \qquad\qquad\qquad\qquad\qquad \text{\textit{gluconate ion}}$$
$$2H_2O_{(l)} + 4NH_{3(aq)} + 2Ag_{(s)}.$$

The same operations with the above-mentioned exposures to the solution **A** and to the mixture of solutions **A** and **B** were performed on other bare GF samples in the absence of ultrasound action or any agitation of these solutions. The latter experiment allowed to evaluate the influence of ultrasound action on the composition, morphology, structure and electrical conductivity of the GF-Ag-US sample. After the electroless deposition, the obtained GF-Ag and GF-Ag-US samples were thoroughly rinsed with water and dried in an oven at 80 °C for 10 h.

Composition, morphology and structure of modified GF

As seen from Fig. 1, the loading of electroless-deposited Ag on the surface of GF-Ag and GF-Ag-US filaments increased in the first 3 min most rapidly. The mass fraction of deposited Ag reached 12.2 and 17.5 wt.% for GF-Ag and GF-Ag-US, respectively. In both cases, after 6 min the mass fraction of Ag in GF-Ag and GF-Ag-US samples changed slightly. This could be related to a relatively fast electroless Ag deposition reaction, when the major part of Ag was formed within the first 6 minutes. The maximal and almost unchangeable loadings of electroless-deposited Ag on the surface of GF-Ag and GF-Ag-US filaments were observed in the deposition time interval from 6 to 24 min. Additionally, it was found that the constant mass fraction of deposited Ag in GF-Ag-US samples, obtained after 6, 12 and 24 min, was approximately 1.6 times greater than in the case of GF-Ag samples. Increasing of the Ag mass fraction onto the filaments of GF-Ag-US samples could be explained by the increased transport rate of reactants into the internal parts of GF and, in general, by acceleration of the deposition process during ultrasonic irradiation of the electroless Ag deposition solution. Therefore, further morphological, compositional and structural investigations were performed only for the GF-Ag and GF-Ag-US samples obtained after 6 min of electroless Ag deposition.

The results of SEM analysis showed that the GF-Ag sample, exposed for 6 min in a non-agitated and not irradiated
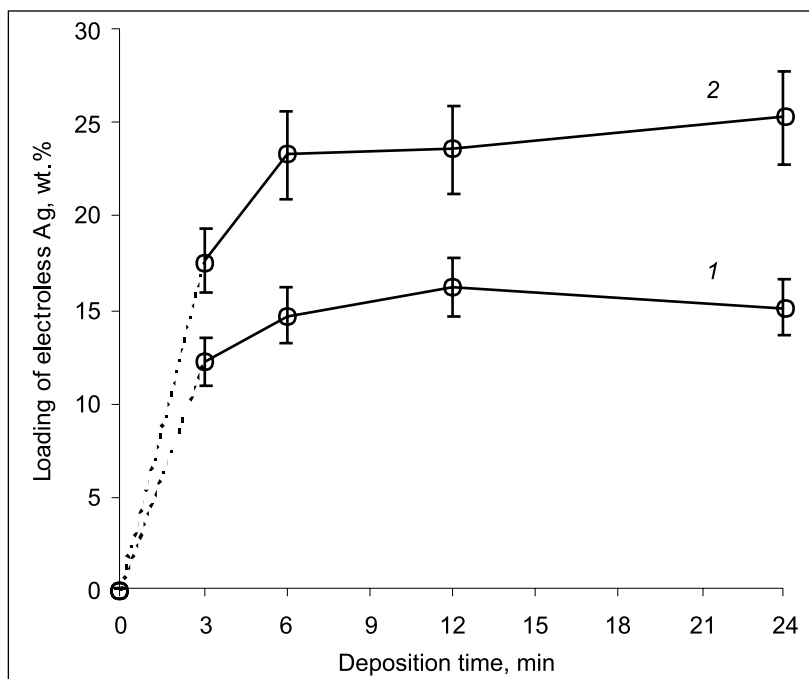
with ultrasound electroless Ag deposition solution, exhibited different surface morphology of Ag, deposited on filaments at the internal and external parts of the samples (Fig. 2a, b).

GF-Ag filaments located at the external part of the sample are fully covered in the dendritic layer of Ag, while GF-Ag filaments at the internal part of the sample exhibit only randomly
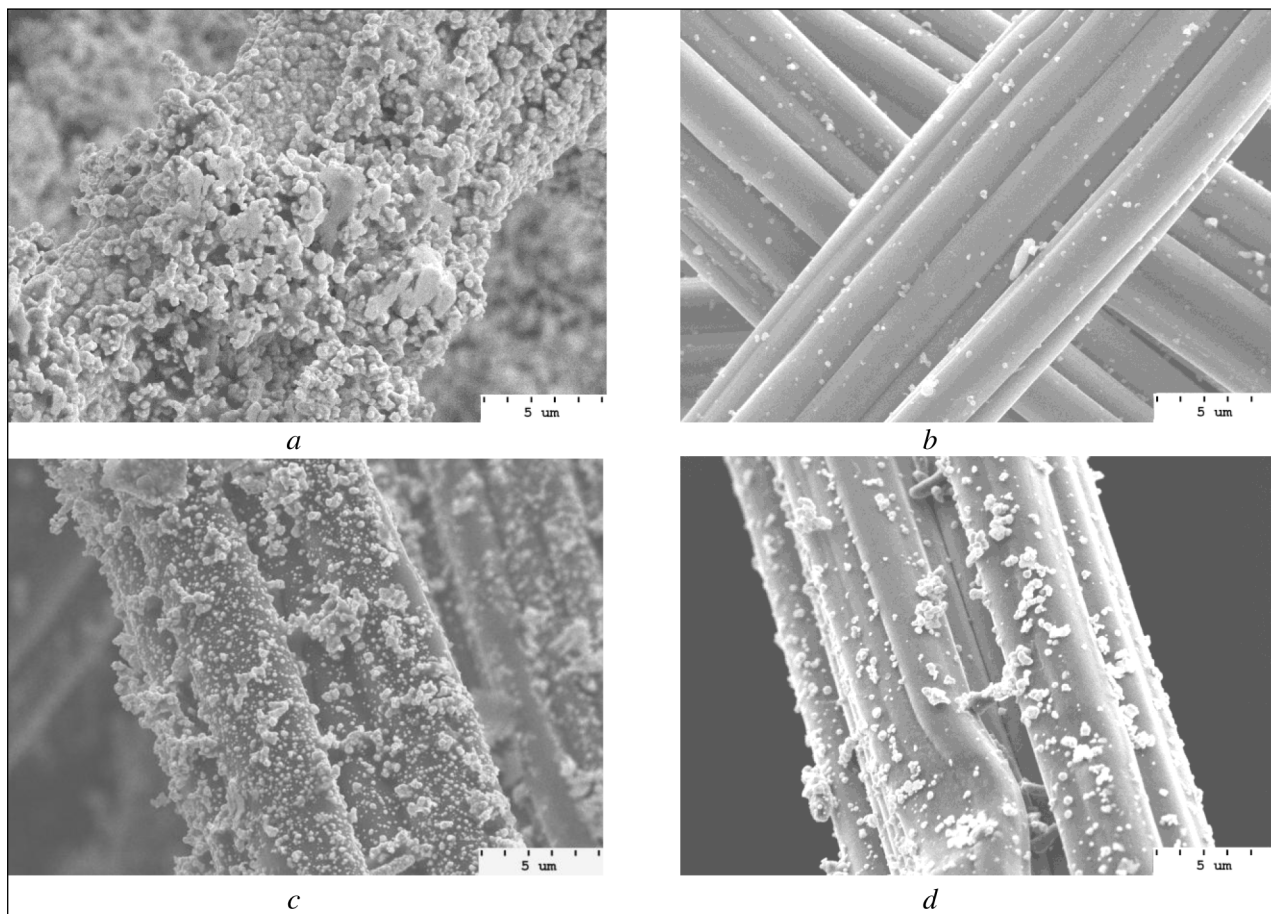

Fig. 2. SEM micrographs of filaments, taken from the external (*a, c*) and internal (*b, d*) parts of GF-Ag (*a, b*) and GF-Ag-US (*c, d*) samples, exposed in electroless Ag deposition solution for 6 min

dispersed individual globular Ag particles of nanometric dimensions (up to 200 nm). When electroless Ag deposition was conducted in the presence of ultrasound action, morphological differences of Ag particles deposited on the external and internal filaments of the GF-Ag-US sample have been reduced greatly (Fig. 2c, d). In both cases, depositions of individual globular Ag particles as well as larger conglomerates of these particles were observed on the surface of filaments of the GF-Ag-US sample. However, the surface concentration of Ag particles was visibly lower onto the internal filaments of the GF-Ag-US sample. Moreover, similar distribution of Ag concentration throughout the internal and external parts of the GF-Ag and GF-Ag-US samples was observed in the results of EDX analysis (Table). When electroless Ag deposition was performed in a non-agitated or non-ultrasonicated solution, the greatest concentration of Ag was found on the surface of external GF-Ag filaments, while the surface of internal filaments exhibited about 100 times lower concentration of Ag particles. In the presence of ultrasound action, a more uniform distribution of Ag concentration, i. e. more uniform deposition of Ag particles, on the surface of the internal and external filaments of the GF-Ag-US sample was obtained. In this case Ag concentration on the surface of internal filaments is only 4.5 times lower in comparison with Ag concentration on the surface of external filaments (Table). This is probably associated with the improved penetration of reactants (mass transport) to the internal filaments and more uniform distribution of the deposited Ag particles in the whole volume of the GF-Ag-US sample. Furthermore, cavitation phenomenon induced by ultrasonic irradiation causes local increases in temperature and pressure at the liquid-solid boundary of the phases. This may lead to an increased number of nucleation and crystallization centres at the surface of GF filaments, as well as the rate of Ag(I) reduction to metallic Ag.

The XRD analysis of the samples showed a significant change in the structure of GF-Ag and GF-Ag-US samples in comparison with bare GF (Fig. 3) In the XRD pattern of bare GF, two broad peaks at 2θ equal to 26.0° and 43.1°, which corresponds to (002) and (100) planes reflections of the graphitic form of carbon [35], are observed (Fig. 3, pattern 1). The appearance of new intense and narrow peaks in the XRD patterns of GF-Ag and GF-Ag-US samples proves the presence of the crystalline Ag phase onto GF filaments. Diffraction peaks at 2θ equal to 38.2°, 44.4° and 64.6° are attributable to (111), (200) and (220) planes, respectively, and they represent the face-centered lattice of pure Ag (PDF-2 card No. 04-0783). Intensity of Ag peaks in the XRD patterns obtained from the internal and external filaments of the GF-Ag-US sample differed slightly. Just more intensive peaks of the Ag phase were observed in the XRD pattern of the external filaments of the GF-Ag-US sample (Fig. 3, patterns 4, 5). Significantly intensive characteristic peaks of the Ag phase were obtained

Table. EDX analysis data of the surface composition of filaments, taken from the external and internal parts of GF-Ag and GF-Ag-US samples, exposed in elecroless Ag deposition solution for 6 min

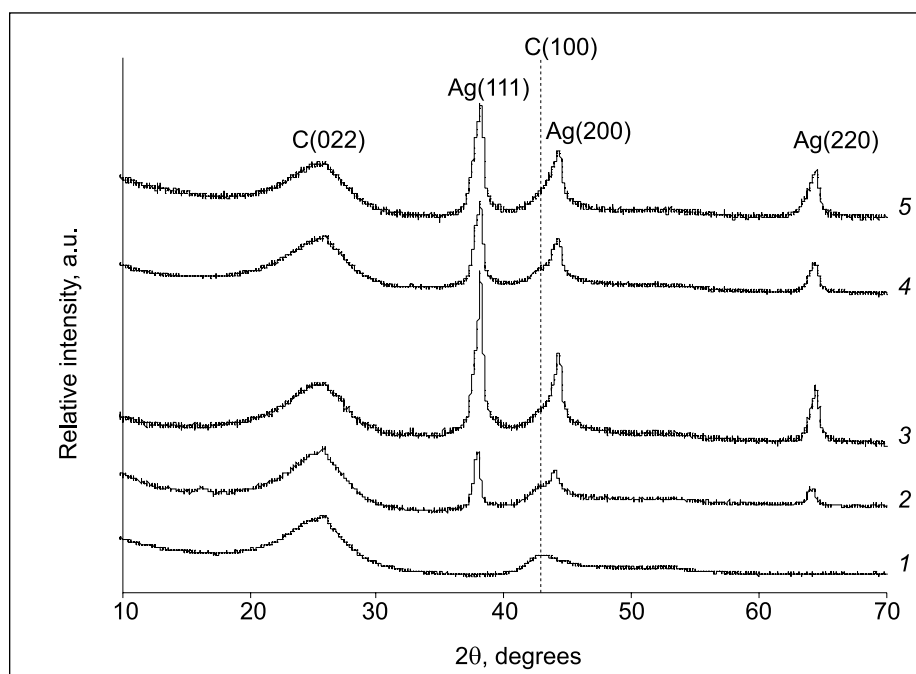| Sample	External filaments of sample			Internal filaments of sample		
	C, at.%	O, at.%	Ag, at.%	C, at.%	O, at.%	Ag, at.%
GF-Ag	66.27	13.24	**20.49**	95.91	3.89	**0.20**
GF-Ag-US	57.08	35.94	**6.98**	92.65	5.79	**1.55**

Fig. 3. XRD patterns of bare GF (*1*), internal (*2, 4*) and external (*3, 5*) filaments of GF-Ag (*2, 3*) and GF-Ag-US (*4, 5*) samples, exposed in electroless Ag deposition solution for 6 min

from the external filaments of the GF-Ag sample (Fig. 3, patterns 2, 3). This is related with the fact that the external filaments of the GF-Ag sample got coated in a thick layer of dendritic Ag (Fig. 2a), and only individual Ag particles were deposited on the surface of external filaments (Fig. 2b). In general, intensity of the characteristic Ag peaks in the XRD patterns correlates with the results of EDX measurements performed to evaluate the distribution of Ag concentration in various parts of the GF-Ag and GF-Ag-US sample, modified in the presence and absence of ultrasound action (Table).

The measurements of the full width at the half maximum (FWHM) of the characteristic Ag peaks at 2θ equal to $38.2°$ (Ag (111)) and $64.6°$ (Ag (220)) have shown that an average crystallite size of elecroless-deposited Ag depends on the impact of ultrasound. When the electroless Ag deposition solution was not ultrasonicated or otherwise agitated, the crystallite sizes of Ag particles deposited on the surface of external and internal filaments of the GF-Ag sample differ slightly and were 14.37 ± 0.25 nm and 13.48 ± 0.17 nm, respectively. The same trend remained when the GF sample was modified with electroless Ag in the presence of ultrasound action. However, the crystallite size of Ag particles deposited on the external and internal filaments of the GF-Ag-US sample were a little bit smaller, i. e. 10.52 ± 0.60 nm and 11.04 ± 0.67 nm, respectively. Thus, the decreasing of the Ag crystallite size was relevant to ultrasonic impact on the crystallisation process of electroless Ag.

Electrical conductivity of modified GF

As seen in Fig. 4, the current–voltage (*I–E*) curves recorded by voltammetric measurements of differential conductance d*I*/d*E* of bare GF, GF-Ag and GF-Ag-US samples have different sloping. The *I–E* curve plotted for the bare GF sample is most sloped in comparison with the appropriate curves recorded for the GF-Ag samples. This indicates that the bare GF has the lowest value of electrical conductivity $\sigma = 6.6 \pm 0.5$ S cm^{-1}. Meanwhile, steeper *I–E* curves were recorded for the GF-Ag and GF-Ag-US samples (Fig. 4, curves 2, 3). It displayed a higher electrical conductivity of the latter samples. The highest value of the electrical conductivity of $\sigma = 10.7 \pm 0.7$ S cm^{-1} was determined for the GF-Ag-US sample. Slightly smaller electrical conductivity of $\sigma = 9.4 \pm 0.8$ S cm^{-1} was obtained for the GF-Ag sample. This is related to the fact that Ag, being a very good conductor, deposited on the surface of GF filaments increased the overall electrical conductivity of GF-Ag and GF-Ag-US composites. Generally, the GF-Ag-US sample exhibited the highest electrical conductivity probably due to more uniform distribution of deposited Ag particles on the surface of filaments in the entire volume of this sample. This in turn leads to the improved homogenous connection between individual filaments in the matrix of the GF-Ag-US composition.

CONCLUSIONS

In summary, modification of GF with electroless-deposited Ag with assistance of ultrasound significantly improved the
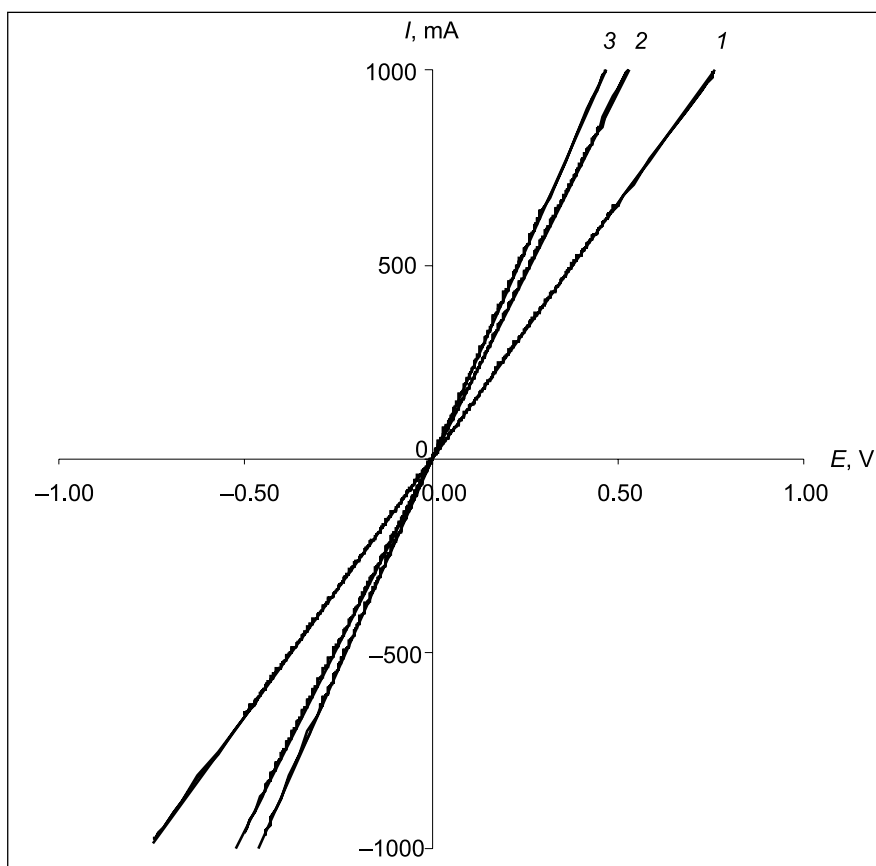

Fig. 4. Current–voltage (*I–E*) curves recorded by voltammetric measurements of differential conductance d*I*/d*E* of bare GF (*1*), GF-Ag (*2*) and GF-Ag-US (*3*) samples, exposed in electroless Ag deposition solution for 6 min

modification process and certain properties of GF-Ag-US. Ultrasound irradiation applied to the electroless Ag deposition solution enabled to increase the loading of Ag on the surface of GF filaments of about 25 wt.%. This is approximately 1.6 times higher compared with the Ag mass fraction of the GF sample modified without ultrasonication. Ultrasonication induced more uniform distribution of crystalline Ag particles deposited in the whole volume of the GF-Ag-US sample. The size of individual globular Ag particles, as well as larger conglomerates of these particles varied in a range from few tens to few hundred nanometres. The crystallite size of Ag particles deposited in the presence of ultrasound action is approximately 11 nm. Thick dendritic coating of electroless Ag with slightly greater crystallites of 14 nm was obtained mainly on the surface of external filaments of the GF-Ag sample.

The homogeneous deposition of Ag on the surface of filaments in the whole volume of the GF-Ag-US sample, as well as up to 1.6 times increased in electrical conductivity, reveals the possibility to use such composition as a flow-through electrode in certain electrochemical systems. The following detailed investigation of electrochemical properties and stability of a GF-Ag-US electrode toward electrocatalytic reduction of hydrogen peroxide will be performed in the nearest future.

References

1. S. Litster, G. McLean, *J. Power Sources*, **130**, 61 (2004).
2. E. M. Belgsir, H. J. Schäfer, *Chem. Commun.*, **5**, 435 (1999).
3. M. S. A. Rahaman, A. F. Ismail, A. Mustafa, *Polym. Degrad. Stabil.*, **92(8)**, 1421 (2007).
4. J. Gonzalez-Garcia, P. Bonete, E. Exposito, V. Montiel, A. Aldaz, R. Torregrosa-Macia, *J. Mater. Chem.*, **9**, 419 (1999).
5. F. Coeuret, E. Oliveira Vilar, E. Bezerra Cavalcant, *J. Appl. Electrochem.*, **32**, 1175 (2002).
6. V. Tricoli, N. Vatistas, P. F. Marconi, *J. Appl. Electrochem.*, **23** (1993).
7. M. Panizza, M. A. Oturan, *Electrochim. Acta*, **56(20)**, 7084 (2011).
8. H. Zhou, H. Zhang, P. Zhao, B. Yi, *Electrochim. Acta*, **51(28)**, 6304 (2006).
9. A. Döner, I. Karci, G. Kardas, *Int. J. Hydrog. Energy*, **37(12)**, 9470 (2012).
10. A. Bauer, E. L. Gyenge, C. W. Oloman, *J. Power Sources*, **167**, 281 (2007).
11. S. Dominguez-Dominguez, J. Arias-Pardilla, A. Berenguer-Murcia, E. Morallon, D. Cazorla-Amoros, *J. Appl. Electrochem.*, **38**, 259 (2008).
12. D. R. Lycke, E. L. Gyenge, *Electrochim. Acta*, **52**, 4287 (2007).
13. W. H. Wang, X. D. Wang, *Electrochim. Acta*, **52**, 6755 (2007).
14. Z. Gonzalez, A. Sanchez, C. Blanco, M. Granda, R. Menendez, R. Santamaria, *Electrochem. Commun.*, **13**, 1379 (2011).
15. B. Li, M. Gu, Z. Nie, et al., *Nano Lett.*, **13**, 1330 (2013).
16. J. H. Zhou, M. G. Zhang, L. Zhao, P. Li, X. G. Zhou, W. K. Yuan, *Catal. Today*, **147S**, S225 (2009).
17. L. Han, S. Tricard, J. Fang, J. Zhao, W. Shen, *Biosens. Bioelectron.*, **43**, 120 (2013).
18. S. Rondinini, A. Vertova, in: C. Comninellis, G. Chen (ed.), *Electrochemistry for the Environment*, Ch. 12, Springer, Berlin (2010).
19. A. A. Isse, S. Gottardello, C. Maccato, A. Gennaro, *Electrochem. Commun.*, **8**, 1707 (2006).
20. G. Flatgen, S. Wasle, M. Lubke, et al., *Electrochim. Acta*, **44**, 4499 (1999).
21. Q. Yi, F. Niu, L. Li, R. Du, Z. Zhou. X. Liu, *J. Electroanal. Chem.*, **654**, 60 (2011).
22. R. Vinodh, D. Sangeetha, *J. Mater. Sci.*, **47**, 852 (2012).
23. S. Maheswari, P. Sridhar, S. Pitchumani, *Electrocatal.*, **3**, 13 (2012).
24. Q. Liu, J. Rosen, Y. Zhou, et al., *Nat. Commun.*, **5**, 1 (2014).
25. T. J. Mason, J. P. Lorimer, *Applied Sonochemistry: The Uses of Power Ultrasound in Chemistry and Processing*, Wiley-VCH (2002).
26. B. G. Pollet, *Int. J. Hydrog. Energy*, **35**, 11986 (2010).
27. A. Gedanken, *Ultrason. Sonochem.*, **11**, 47 (2004).
28. V. Saez, T. J. Mason, *Molecules*, **14**, 4284 (2009).
29. Y. Lu, S. Jiang, Y. Huang, *Surf. Coat. Technol.*, **204**, 2829 (2010).
30. M. Schlesinger, M. Paunovic, *Modern Electroplating*, 5th edn., John Wiley & Sons, Inc., Hoboken, New Jersey (2010).
31. B. D. Cullity, *Elements of X-ray Diffraction*, Addison-Wesley Publishing Company Inc. (1978).
32. K. Wang, K. Chizari, Y. Liu, et al., *Appl. Catal. A*, **392**, 238 (2011).
33. P. Zhao, H. Zhang, H. Zhou, B. Yi, *Electrochim. Acta*, **51(6)**, 1091 (2005).
34. B. Sun, M. S. Kazacos, *Electrochim. Acta*, **37(13)**, 2459 (1992).
35. Y. Wang, J. Cao, Y. Zhou, J. H. Ouyang, D. Jia, L. Guo, *J. Electrochem. Soc.*, **159(5)**, A579 (2012).

Brigita Macijauskienė, Egidijus Griškonis

**GRAFITO VELTINIO BESROVIS MODIFIKAVIMAS
SIDABRU VEIKIANT ULTRAGARSUI**

I. Sudėtis, morfologija, struktūra ir elektrinis laidumas

Santrauka

Darbe tirta ultragarso įtaka grafito veltiniui modifikuoti sidabru naudojant besrovį nusodinimo būdą. Gravimetriškai nustatyta, kad grafito veltinio siūlelių paviršiuje nusėdusio Ag masės dalis (%) priklauso nuo ultragarso poveikio ir ji yra apie 1,6 karto didesnė nei modifikuojant grafito veltinį be ultragarso poveikio. Grafito veltinio bandinių, modifikuotų sidabru esant ir nesant ultragarso poveikiui, vidinių ir išorinių siūlelių paviršiaus morfologija, sudėtis ir struktūra buvo nustatytos atitinkamai naudojant skenuojančią elektroninę mikroskopiją, rentgeno spindulių energijos dispersinę spektroskopiją bei rentgeno spindulių difrakcinę analizes. Pastebė- ta, jog veikiant ultragarsui ant grafito veltinio siūlelių nusodinamos nanometrinių matmenų Ag dalelės, kurių forma artima sferoidams, daug tolygiau pasiskirsto visame grafito veltinio tūryje. Nenaudo- jant ultragarso ant grafito veltinio siūlelių nusodinto smulkiakris- talinio Ag kristalitų dydis yra apie 14 nm, o besrovio sidabravimo tirpalą veikiant ultragarsu nusodinto Ag kristalitų dydis sumažėjo iki 11 nm. Tolygus grafito veltinio siūlelių padengimas Ag dalelėmis visame bandinio tūryje padidino jo elektrinį laidį iki 10,7 $S \cdot cm^{-1}$, ši vertė yra apie 1,6 karto didesnė, palyginti su nemodifikuoto grafito veltinio elektriniu laidžiu.